EARTHQUAKE ENGINEERING AND STRUCTURAL DYNAMICS, VOL. 26, 269–288 (1997)

SEISMIC MONITORING OF A BRIDGE: ASSESSING DYNAMIC CHARACTERISTICS FROM BOTH WEAK AND STRONG GROUND EXCITATIONS

CHIN-HSIUNG LOH* AND ZHENG-KUAN LEE†

Department of Civil Engineering, National Taiwan University, Taipei, Taiwan 10764, R.O.C.

SUMMARY

An array of 24 strong-motion accelerometers produced records for the New-Lian River Bridge, a five-span continuous bridge, during 25 February 1995 earthquake (weak motion) and 25 June 1995 earthquake (strong motion). This paper describes the application of linear discrete-time system identification methodology to the array of strong-motion measurements, in order to assess seismic response characteristics of the bridge. The structural system identification will concentrate not only on the global identification but also on the local structural system identification. Results of this application show that: (1) weak and strong ground excitation will induce significant differences on the dynamic response of the bridge; (2) linear models provide an excellent fit to the measured motions of the bridge from the records of these two seismic events; (3) the rigid-body rocking of the bridge pier during strong shaking is significant and cannot be ignored during identification; (4) the transverse motion at mid-span of the bridge is controlled by the quasi-static response from the boundary system and this phenomenon is quite significant during strong ground excitation. Also, systematic estimates of modal damping ratio and equivalent assessments of pier stiffness developed in the bridge during earthquake are discussed.

KEY WORDS: finite element modelling; Kalman filtering technique; linear discrete-time identification

INTRODUCTION

Past earthquakes have often caused extensive damage to bridges, resulting in significant inconvenience and economic loss to the surrounding communities.[1–3] In addition, there has been significant activity among earthquake engineers directed toward gaining further insight into the behaviour of bridges during earthquakes. These activities have entailed qualitative observations and interpretations of the behaviour of bridges during past earthquakes. One of the example is the Meloland Road Overpass which has been studied by Douglas,[4] Wilson,[5] and Werner.[6] It is clear that strong-motion measurements of actual bridge response, when evaluated using established system identification techniques, can provide important quantitative information concerning the seismic response of bridges.

On 23 February and 25 June 1995, two earthquakes with magnitude 5·77 and 6·50, respectively, occurred at the east coast of Taiwan (Figure 1). Among the accelerograms obtained during these two earthquakes were those measured at the New-Lian River Bridge (NLRB), a continuous five-span prestressed box-girder bridge located at the northwest coast of Taiwan.

The NLRB had been instrumented with an array of 24 strong motion accelerometers along its deck, at its abutments and at a nearby free-field location (Figure 2). All of these instruments were triggered during 23 February 1995 earthquake, and 25 June 1995 earthquake, providing one of the most extensive array of strong motion measurements. Table I shows the recorded maximum acceleration at each of the accelerograms. The event of 25 June 1995 earthquake induced significant response at some of the measurement points.

* Professor
† Graduate student

CCC 0098–8847/97/020269–20

Received 12 March 1996
Revised 11 September 1996

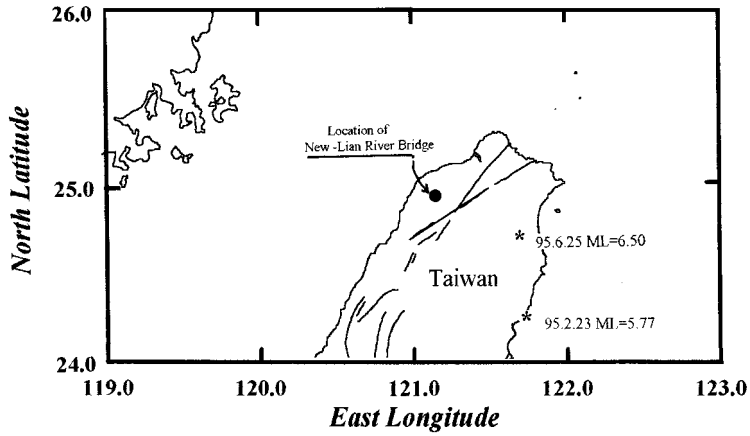

Figure 1. Epicentres of two earthquakes and the location of New-Lian River Bridge

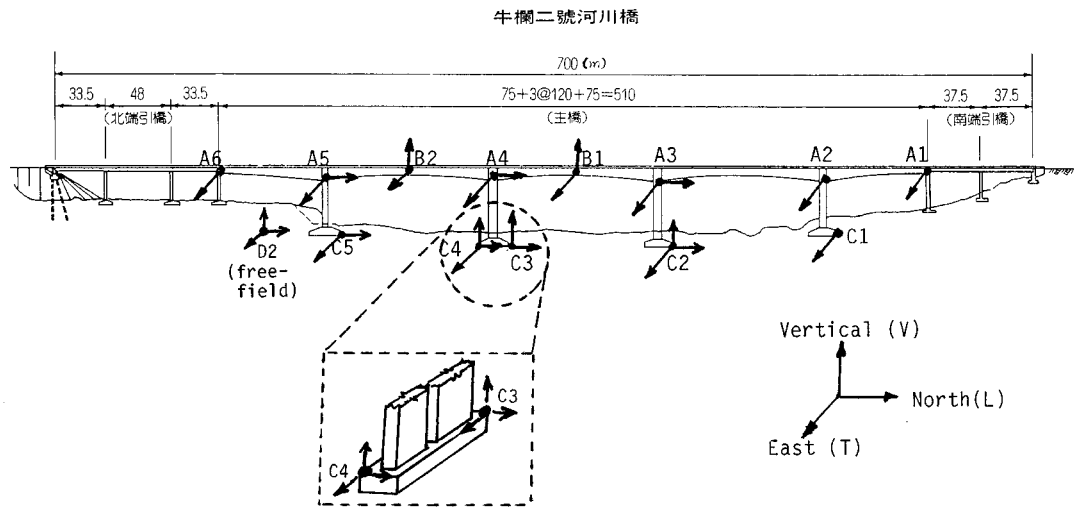

Figure 2. Instrumentation layout at New-Lian River Bridge (provided by Central Weather Bureau)

Presented in this paper is a procedure to estimate dynamic characteristics, such as modal damping, natural frequencies and stiffness of pier–girder system, directly from the recorded motion of a well-instrumented bridge. The procedure for the local system identification is used to identify the differences in dynamic characteristics of the bridge girder and pier from these two earthquake response data. This study consisted of main parts that entailed (1) development of both global and local system identification methodology suitable for evaluation of bridge response data; (2) application of the methodology to the recorded array data in order to evaluate the seismic response characteristics of the NLRB; (3) systematic estimates and discussion of pier stiffness in the bridge during earthquakes are provided; (4) the influence of quasi-static response on local structural identification is discussed from the response data of two seismic events.

PRELIMINARY ANALYSIS AND DATA PROCESSING

The NLRB was instrumented in November 1994 by Central Weather Bureau. This instrumentation comprise single-axis, two-axes and triaxial force-balanced accelerometer packages with 16-bit resolution which makes

Table I. Recorded maximum peak accelerations for 1995-2-23 and 1995-6-25 earthquakes from strong motion instrumentations at New-Lian River bridge

	Earthquake: 23 February 1995 $M = 5{\cdot}77$ $D = 21{\cdot}7$ km			Earthquake: 25 June 1995 $M = 6{\cdot}50$ $D = 39{\cdot}9$ km		
	EW	NS	VR	EW	NS	VR
C1	16	—	—	120	—	—
C2	19	13·4	8·3	125	131	48
C3	—	—	9·5	—	107	58
C4	18	12·7	8·7	104	101	40
C5	15	15·1	—	145	78	—
A1	58	—	—	511	—	—
A2	28	—	—	188	—	—
A3	51	19·2	—	381	212	—
A4	48	—	—	343	166	—
A5	43	14·9	—	223	201	—
A6	86	—	—	693	—	—
B1	83	—	54	689	—	960
B2	60	—	60	521	—	556

Unit: Gal
EW: Corresponding to transverse direction
NS: Corresponding to longitudinal direction

the apparatus capable of recording high-resolution ground motion and structural response within $\pm 2g$ over a nominal frequency range of 0 to 100 Hz and with a pre-event and post-event memory. This bridge instrumentation is maintained by the Seismological Observation Center, Central Weather Bureau. Figures 3(a) and 3(b) show the recorded accelerograms at some of the locations of this bridge from the two seismic events. All the recorded accelerograms have their synchronization of the motion automatically. It has to be pointed out that 25 June 1995 earthquake caused large accelerations at some observation points of the bridge. For example, in the vertical direction at station B1, the response data shows the peak acceleration of 960 gals.

The Fourier amplitude spetrum of the recorded accelerations along the bridge deck in transverse direction was analysed first. The fundamental mode of vibration in the transverse direction along the bridge deck was identified. One can select the peak amplitude of Fourier spectrum and check the phase at this particular frequency to identify the mode shape. Figure 4(a) shows the identified fundamental mode shape at $f = 9{\cdot}173$ rad/s in transverse direction from 23 February 1995 earthquake data, and Figure 4(b) shows the mode shape at $f = 8{\cdot}543$ rad/s in transverse direction from 25 June 1995 earthquake data. It is found that a rigid body translational mode was included in the identified mode shape in Figure 4(b). The rigid-body rocking of the abutment was observed from the stronger excitation of 25 June 1995 earthquake. The identified mode shape corresponds to the third mode of the bridge system (as shown in Figure 5 by using analytical treatment). Detail system identification will be performed from the local structural system identification to determine the dynamic characteristics of the NLRB.

MULTIPLE INPUTS STRUCTURAL SYSTEM IDENTIFICATION

Background of dynamic system in discrete-time domain

A linear discrete-time model is generally described as

$$y(t) = -\sum_{i=1}^{n} a_i y(t-i) + \sum_{i=1}^{m} b_i u(t-d-i) \tag{1}$$

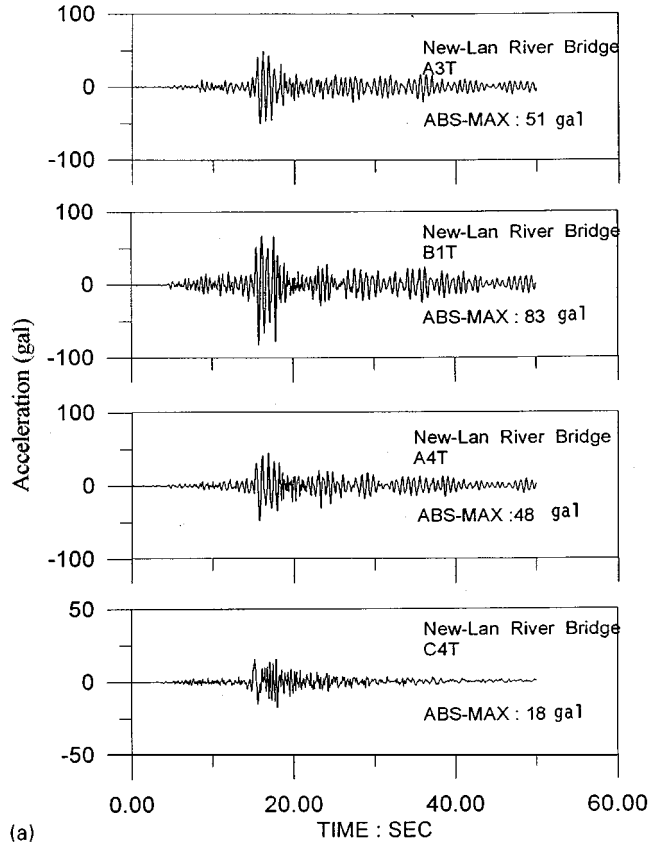

Figure 3. (a) Acceleration records of stations A3, B1, A4 and C4 in transverse direction for 1995-2-23 earthquake

in which d corresponds to a time delay that is an integer multiple of the sample period, $y(t)$ and $u(t)$ are output and input with a certain sampling period. If the delay operator Z^{-1} is used that satisfies the following relation:[7]

$$Z^{-1}y(t) = y(t-1) \quad \text{and} \quad Z^{-d}y(t) = y(t-d) \tag{2}$$

then equation (1) can be written as

$$A(Z^{-1})y(t) = Z^{-d}B(Z^{-1})u(t) \tag{3}$$

in which

$$\begin{aligned} A(Z^{-1}) &= 1 + a_1 Z^{-1} + a_2 Z^{-2} + \cdots + a_n Z^{-n} \\ B(Z^{-1}) &= b_1 + b_1 Z^{-1} + b_2 Z^{-2} + \cdots + b_m Z^{-m} \end{aligned} \tag{4}$$

$A(Z^{-1})$ and $B(Z^{-1})$ are polynomials in Z^{-1} of degree n and m, respectively. The corresponding identification problem consists of determining the modal structure and parametric estimation of the polynomials in equation (4) if the system can be expressed in the linear discrete-time domain. For the identification of dynamic properties of structural seismic response, three transfer function models can be used in the discrete-time domain for linear time-invariant system.

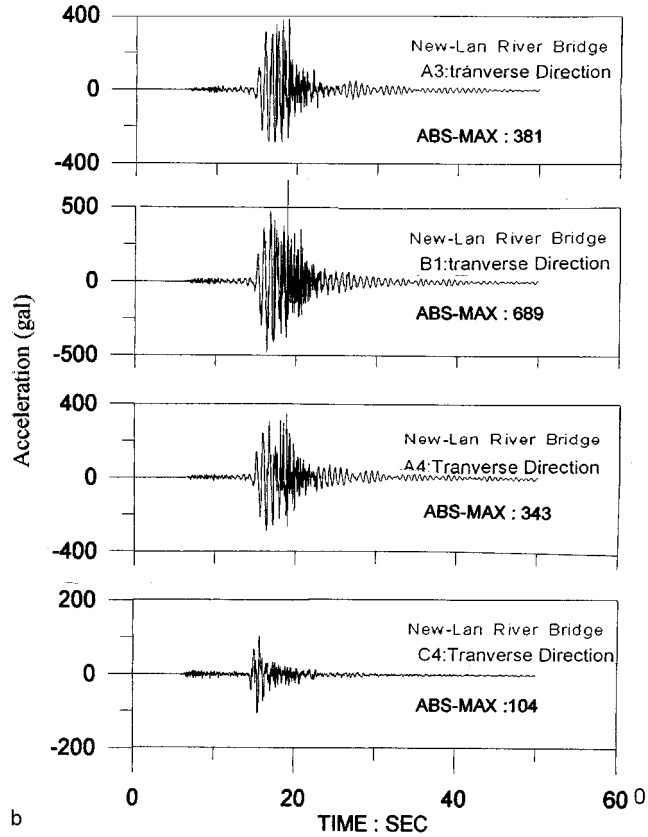

Figure 3. (b) Acceleration records of stations A3, B1, A4 and C4 in transverse direction for 1995-6-25 earthquake

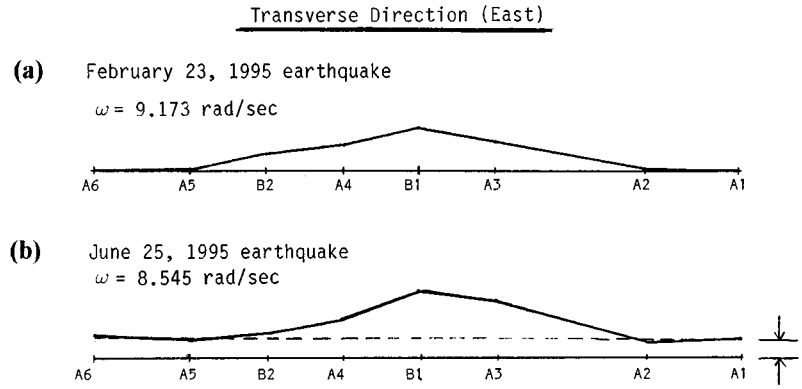

Figure 4. Identification of the fundamental mode shape in transverse direction along the 5-span bridge girder; (a) from the 1995-2-23 earthquake, (b) from the 1995-6-25 earthquake (——) the quasi-static response was observed

(a) ARX model (autoregressive model with noise):

$$y(t) = \frac{B(Z^{-1})}{A(Z^{-1})}u(t) + \frac{1}{A(Z^{-1})}e(t) \tag{5}$$

(b) Output-error model:

$$y(t) = \frac{B(Z^{-1})}{A(Z^{-1})}u(t) + e(t) \tag{6}$$

(c) ARMAX model:

$$y(t) = \frac{B(Z^{-1})}{A(Z^{-1})}u(t) + \frac{C(Z^{-1})}{A(Z^{-1})}e(t) \tag{7}$$

These three models are parameterized as modal structures, using a parameter vector $\hat{\theta} = \langle -a_1, -a_2, \ldots, b_1, b_2, b_3, \ldots \rangle$. In this study the identification of a linear system by using the output-error model was considered as the determination of the transfer function between two measurements. It becomes equivalent to the determination of the coefficients a_k and b_k in equation (1). The maximum likelihood method can be used to identify the modal parameters.

Once the parameters of the model (output-error model) are identified, it can be converted to parallel form realization as follows:

(1) The poles of the transfer function, $\mathbf{H}_i(Z) = B_i(Z^{-1})/A_i(Z^{-1})$, between the ith input and output of the model are in complex-conjugate pairs, and $\mathbf{H}_i(Z)$ can be put into the following form realization by using partial transfer expansion:

$$\mathbf{H}_i(Z) = \sum_{j=1}^{n/2} H_{ij}(Z) = \sum_{j=1}^{n/2} \frac{C_{0j} + C_{1j}Z}{(Z - \alpha_j)(Z - \alpha_j^*)} \tag{8}$$

in which n is the order of the model (it is an even number). α_i and α_j^* are the pair of complex conjugate poles, C_{0j} and C_{1j} are the real coefficients. In equation (8), a total of $n/2$ modes is considered.

(2) Each $H_{ij}(Z)$ in equation (8) is the transfer function of the single-degree-of-freedom dynamic system, which is equivalent to that of a simple-damped oscillator in the frequency domain. The denominator of $H_{ij}(Z)$ gives the damping and the natural frequency of the oscillator. This simple damped oscillator corresponds to uniform samples at sample interval Δt and can be expressed as

$$y_t + \sum_{k=1}^{2} a_k y_{t-k} = \sum_{k=1}^{2} b_k f_{t-k} \tag{9}$$

with which the transfer function of equation (9) is expressed as

$$H(Z) = \frac{b_1 Z + b_2 Z^2}{1 + a_1 Z + a_2 Z^2} \tag{10}$$

(3) For a single-degree-of-freedom system with equation of motion expressed as follows:

$$\ddot{y}(t) + 2\xi_0\omega_0\dot{y}(t) + \omega_0^2 y(t) = f(t) \tag{11}$$

The system transfer function between excitation $f(t)$ and the relative displacement output $y(t)$, in terms of Laplace transformation, can also be expressed as

$$H(S) = \frac{\omega_0^2}{S^2 + 2\xi_0\omega_0 S + \omega_0^2} \tag{12}$$

Comparing equations (10) and (12), the coefficients in the discrete-time model can be related to the physical parameters ω_0 and ξ_0 [8]

$$b_1 = 1 - \alpha\left(\beta - \frac{\xi_0\omega_0}{\omega'}\gamma\right), \qquad b_2 = \alpha^2 + \alpha\left(\frac{\xi_0\omega_0}{\omega'}\gamma - \beta\right), \qquad a_1 = -2\alpha\beta \quad \text{and} \quad a_2 = \alpha^2 \tag{13}$$

where

$$\omega' = \omega_0\sqrt{1 - \xi_0^2}, \qquad \alpha = \exp(-\xi_0\omega_0\Delta t), \qquad \beta = \cos(\omega_0\Delta t), \qquad \gamma = \sin(\omega_0\Delta t)$$

and Δt is the sampling time, from which the natural frequency and damping ratio of the linear SDOF system can be identified.

Identification of multiple-supported structural system

In the dynamic analysis of linear systems to multi-support excitations, such as the bridge system, it is common to decompose the response into quasi-static component ($\mathbf{X}^{s}(t)$) and dynamic components ($\mathbf{X}^{d}(t)$). A generic response quantity of interest $\mathbf{Z}(t)$ (e.g. a modal displacement, an internal force, stress or strain component), in general, can be expressed as a linear function of the nodal displacements, i.e.,

$$\mathbf{Z}(t) = \mathbf{q}^{T}\mathbf{X}(t) = \mathbf{q}^{T}(\mathbf{X}^{s}(t) + \mathbf{X}^{d}(t)) \tag{14}$$

where $\mathbf{q}$ is a response transfer vector. In terms of the normalized modal responses, the generic response $\mathbf{Z}(t)$ of ith node, $z_i(t)$, is expressed as[9]

$$z_i(t) = \sum_{k=1}^{m} a_k^i u_k(t) + \sum_{k=1}^{m}\sum_{j=1}^{n} b_{kj}^i s_{kj}(t) \tag{15}$$

where $u_k(t)$ is the kth prescribed support displacement, $s_{kj}(t)$ defines a normalized modal response of jth mode to kth support input motion, a_k^i and b_{kj}^i, are functions of the structural properties.

Equation (15) can be expressed as the multi-input/single-output discrete-type linear model:

$$z(t) = \frac{B_1(q)}{A_1(q)}u_1(t) + \frac{B_2(q)}{A_2(q)}u_2(t) + \cdots + \frac{B_{nu}(q)}{A_{nu}(q)}u_{nu}(t) + \sum_{k=1}^{nu} C_k u_k(t-d) + e(t) \tag{16}$$

where $A(q) = 1 + a_1 z^{-1} + a_2 z^{-2} + \cdots + a_n z^{-n_a}$ with order n_a and $z^{-1}z(t) = z(t-1)$, $z^{-d}z(t) = z(t-d)$ and $B_1(q), \ldots, B_{nu}(q)$ are also polynomials in q^{-1} with respect to each input with order $n_{k_1}, \ldots, n_{k_{nu}}$, respectively. C_i corresponds to the contribution of quasi-static components.

Case study of multi-input/single-output identification

In the beginning, the seismic response data of NLRB from 23 February 1995 earthquake was analysed. First, consider the transverse motion of node B1 as output and the abutment motion of stations C2 and C4 as inputs. The quasi-static contributions from supports were also considered. By using the discrete-time output-error model of order 4, as shown in equation (16), the model parameters can be estimated. The natural frequency and damping ratio of each mode can also be calculated by using equation (13). Table II shows the

Table II. Identified natural frequencies, damping ratios and quasi-static term using B1 as output and C2 and C4 as inputs (transverse motion)

B1/C2 (transverse dir.)			B1/C4 (transverse dir.)			
		Earthquake: 23 Feb. 1995				Error
ω	ξ (%)	a_j	ω	ξ	a_j	(%)
8·846	0·49		10·24	0·6		
		0·545			0·484	4·0
28·17	0·88		25·704	2·56		
		Earthquake: 25 June 1995				
9·037	0·91		8·89	0·63		
		0·436			0·582	3·8
11·76	0·90		12·47	1·02		

comparison of the estimated natural frequencies and damping ratios from the two earthquake data. The identified natural frequencies, 9 and 12 rad/s, correspond to the 3rd and 7th modes of the designed vibration system (shown in Figure 5). Because the transverse motion of B1 point was selected as output for the identification, only the 3rd mode and 7th mode natural frequencies can be identified, and the first mode (longitudinal mode), second mode and 6th mode (vertical mode) cannot be identified. While B1 point is located at the node point of the 4th and 5th modes, no such vibration modes can be identified. Consider the vertical vibration of node B1 as output and the abutment vertical motion of station C2 and C4 as input, Table III shows the results of identification. The identified natural frequency, 11·5 rad/s, corresponds to the 6th mode of the design vibration system. The higher mode can also be identified.

For the analysis of transverse motion of station B1, it is also possible to use the recorded transverse motion of nodes A3 and A4 from the boundary of the girder as inputs. Equation (16) can also be applied to identify the natural frequency and damping ratio of the system and the quasi-static contribution from the boundary. As a matter of fact the input motions in this case contain not only the recorded transverse motion of nodes A3 and A4, but also some unmeasured vibration from these two boundaries, such as rotation motion. For a system subjected to small earthquake excitations, if only the transvese motions from nodes A3 and A4 are considered as multiple inputs, good results of identification can still be obtained. Table IV shows the result of

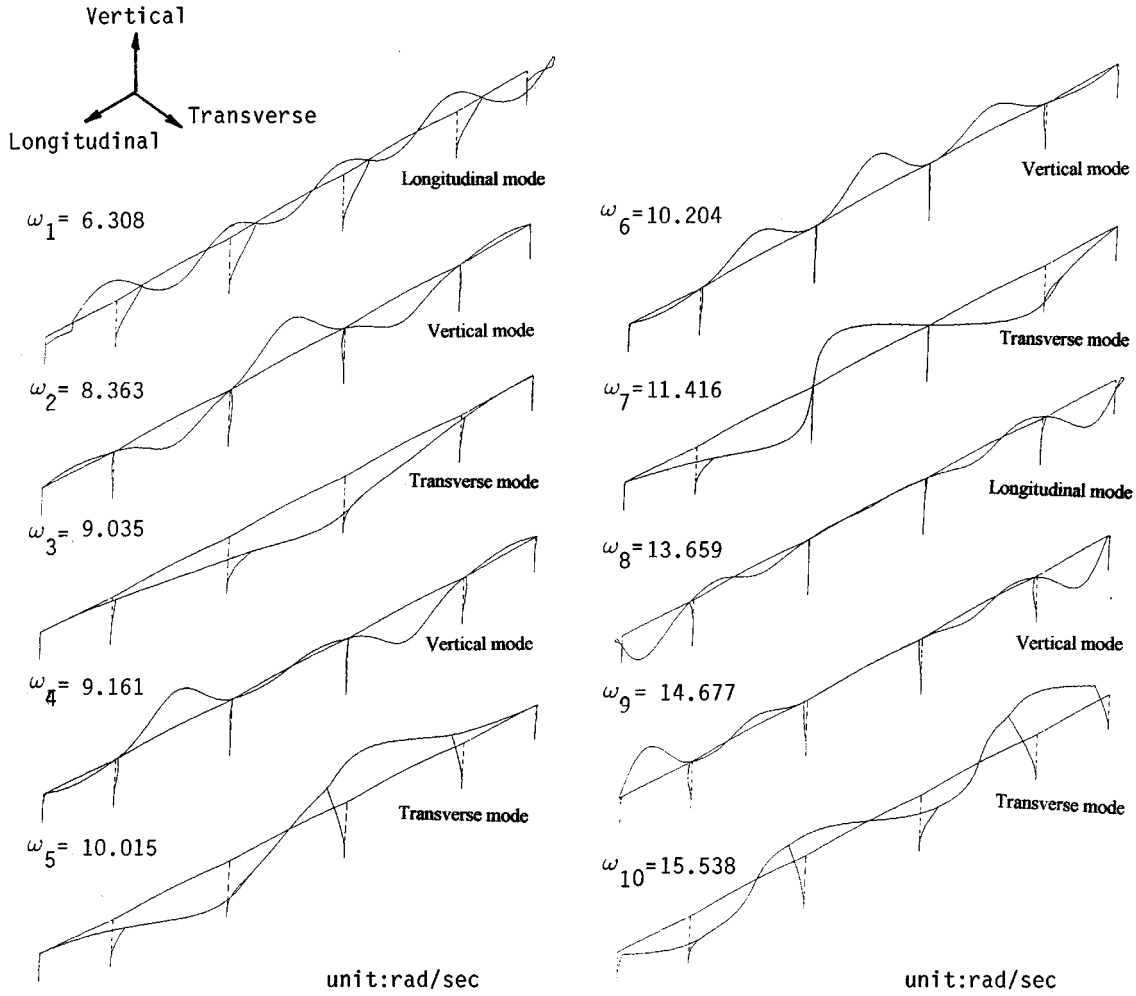

Figure 5. Calculated first 10 mode shapes of the New-Lian River Bridge

Table III. Identified natural frequencies, damping ratios and quasi-static term using B1 as output and C2 and C4 as inputs (vertical motion)

B1/C2 (vertical dir.)			B1/C4 (vertical dir.)			
		Earthquake: 23 Feb. 1995				Error
ω	ξ (%)	a_j	ω	ξ (%)	a_h	(%)
11·54	0·58	0·91	12·55	0·59	0·09	4·5
		Earthquake: 25 June 1995				
11·09	2·65		11·19	0·67		
11·52	1·40	−0·67	11·54	0·91	1·49	5·0
23·95	2·62		23·94	0·41		

Table IV. Identified natural frequency, damping ratio and quasi-static term from the girder segment A3–A4 during 1995-2-23 earthquake. Two different orders of output-error model are used: (a) for order of (2, 2), (b) for order of (4, 4)

	B1/A3			B1/A4			Error
Case a: (2, 2)	ω	ξ (%)	a_j	ω	ξ (%)	a_h	(%)
$d = 0$	12·45	2·3	0·41	12·56	1·3	0·60	1·58
$d = -1$	12·58	2·0	0·45	12·61	1·1	0·57	1·59
Case b: (4, 4)							
$d = 0$	12·51	2·1		12·58	1·22	0·59	1·41
			0·45				
	22·99	7·5		—	—	—	
$d = -1$	12·52	2·43	0·49	12·59	1·23		1·31
						0·56	
	—	—	—	14·55	1·6		

Table V. Identified natural frequency, damping ratio and quasi-static term from the girder segment A4–A5 during 1995-2-23 earthquake. Two different orders of output-error model are used: (a) for order of (2, 2), (b) for order of (4, 4)

	B2/A4			B2/A5			Error
Case a: (2, 2)	ω	ξ (%)	a_j	ω	ξ (%)	a_h	(%)
$d = -1$	13·77	3·65	0·21	13·77	3·65	0·79	3·4
Case b: (4, 4)							
$d = 0$	13·83	1·73		13·86	1·48		2·8
			0·18			0·83	
	16·07	0·89		15·96	1·1		

identified modal parameters of girder segment A3–A4 in transverse motion. The root-mean square error of the predicted response of node B1 is within 2 per cent. Similar results can be obtained by considering the transverse motion of node B2 as output and nodes A5 and A4 as inputs, and the result is shown in Table V. Generally speaking, the contributions of boundary excitations for each local structural system in actual structural system is very complicated, and sometimes it is not enough to use a portion of the boundary

excitations as inputs. In the weak motion the contribution of the transverse motion of boundary excitations to the transverse motion of mid-span is significant and the use of such a limited number of inputs can provide enough input information for identification. The result from Tables IV and V corresponded to the 7th mode in Figure 5 (the 3rd mode cannot be identified because of small contribution).

THE LOCAL STRUCTURAL SYSTEM IDENTIFICATION

By using substructural analysis one can focus the identification to a local arbitrary subsystem within the complete structural system. Without loss of generality, the complete structural system can be divided into two substructures, the smaller substructure is referred to as the secondary (s-system) and the larger as the primary (p-system). These two subsystems have a common boundary which is denoted as b-system, as shown in Figure 6. If our interest is in the identification of the structural parameters of a local subsystem, the equation of motion corresponding to the substructure (s-system) will be considered,[10] i.e.,

$$\mathbf{M}_{ss}\ddot{\mathbf{U}}_s(t) + \mathbf{C}_{ss}\dot{\mathbf{U}}_s(t) + \mathbf{K}_{ss}\mathbf{U}_s(t) = \mathbf{F}_s(t) - \mathbf{F}_{sb}(t) \tag{17}$$

where

$$\mathbf{F}_{sb}(t) = \mathbf{M}_{sb}\ddot{U}_b(t) + \mathbf{C}_{sb}\dot{U}_b(t) + \mathbf{K}_{sb}U_b(t) \tag{17a}$$

Equation (17) gives the response of the internal DOFs of the subsystem due to the external force $\mathbf{F}_s(t)$, acting at the internal DOFs and the boundary force, $\mathbf{F}_{sb}(t)$, resulting from the motion of the boundary DOFs. M_{ss}, C_{ss}, K_{ss} are the mass matrix damping matrix and stiffness matrix of the subsystem.

To illustrate the local identification method, a T-section of a bridge system (the T-section includes girder and pier system) will be analysed, as shown in Figure 7. The equation of motion of mass m_i (mass lumped at the top of the pier) in the transverse direction can be written as

$$\begin{aligned} m_i\ddot{u}_i + c_i\dot{u}_i + k_iu_i = &- m_i\ddot{u}_g(t) - c_{i+1}(\dot{u}_i - \dot{u}_{i+1}) - k_{i+1}(u_i - u_{i+1}) \\ &- c_{i-1}(\dot{u}_i - \dot{u}_{i-1}) - k_{i-1}(u_i - u_{i-1}) \end{aligned} \tag{18}$$

where k_i and c_i are the stiffness and damping of bridge pier in transverse direction, k_{i+1} and c_{k+1} are the girder stiffness and damping between mass i and mass $i+1$, k_{i-1} and c_{i-1} are the girder stiffness and damping between mass i and mass $i-1$ in transverse direction. Equation (18) can be simplified in the following form:

$$\ddot{u}_i + \tilde{c}_i\dot{u}_i + \tilde{k}_iu_i = -\ddot{u}_g(t) - \tilde{c}_{i+1}\dot{z}_{i+1} - \tilde{k}_{i+1}z_{i+1} - \tilde{c}_{i-1}\dot{z}_{i-1} - \tilde{k}_{i-1}z_{i-1} \tag{19}$$

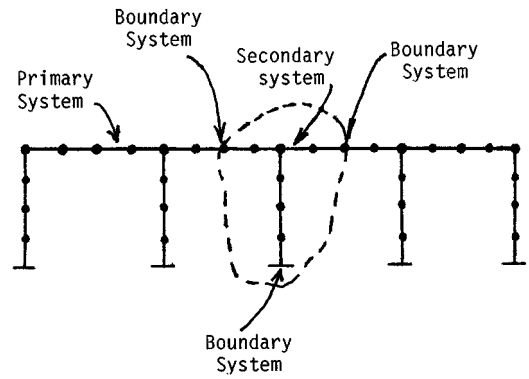

Figure 6. A bridge structure divided into two substructures (primary system and secondary system) with common boundary

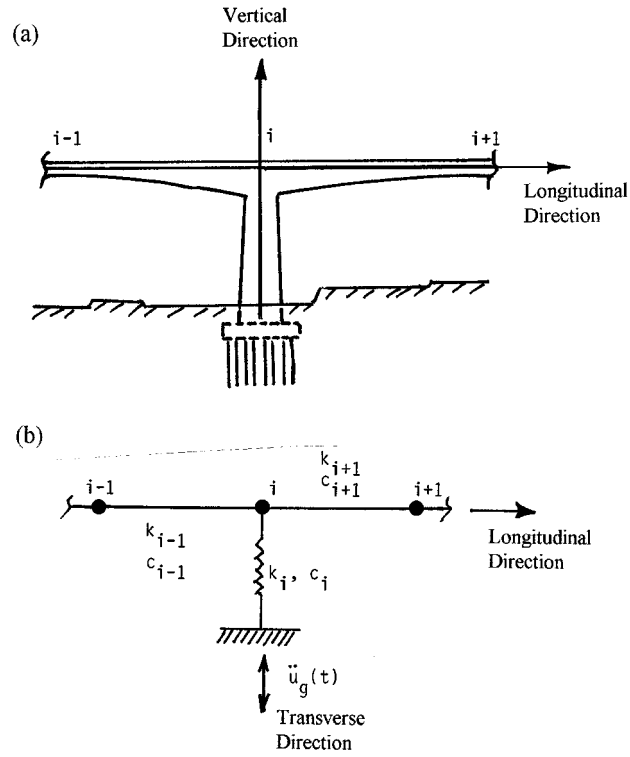

Figure 7. (a) A bridge-girder substructure system, (b) lumped mass model indicates model parameters (stiffness and damping) in each element

where $z_{i+1} = u_i - u_{i+1}$ and $z_{i-1} = u_i - u_{i-1}$, and

$$\tilde{k}_i = \frac{k_i}{m_i}, \qquad \tilde{c}_i = \frac{c_i}{m_i}, \qquad \tilde{c}_{i+1} = \frac{c_{i+1}}{m_i}, \qquad \tilde{k}_{i+1} = \frac{k_{i+1}}{m_i}$$
$$\tilde{c}_{i-1} = \frac{c_{i-1}}{m_i}, \qquad \tilde{k}_{i-1} = \frac{k_{i-1}}{m_i} \tag{19a}$$

The objective of the local identification is to describe completely the properties of the substructure by identifying the substructural parameters. Therefore, the current identification problem consists of finding the optimal estimates of the unknown coefficients $\tilde{c}_i, \tilde{k}_i, \tilde{c}_{i+1}, \tilde{k}_{i+1}, \tilde{c}_{i-1}$ and $\tilde{k}_{i-1}$. Select $u_i(t)$ and $\dot{u}_i(t)$ as the state variables, the state vector can be written as

$$\begin{aligned} \vec{\mathbf{X}} &= \{u_i, \dot{u}_i, \tilde{c}_i, \tilde{k}_i, \tilde{c}_{i-1}, \tilde{k}_{i-1}, \tilde{c}_{i+1}, \tilde{k}_{i+1}\}^{\mathrm{T}} \\ &= \langle x_1, x_2, x_3, x_4, x_5, x_6, x_7, x_8 \rangle^{\mathrm{T}} \end{aligned} \tag{20}$$

The state equation in the form of a differential equation can be derived as

$$\frac{\mathrm{d}\vec{\mathbf{X}}}{\mathrm{d}t} = \begin{Bmatrix} \dot{u}_i \\ \ddot{u}_i \\ 0 \\ \vdots \\ 0 \end{Bmatrix} = \begin{Bmatrix} x_2 \\ -x_3 x_2 - x_4 x_1 - x_5 \dot{z}_{i-1} - x_6 z_{i-1} - x_7 \dot{z}_{i+1} - \dot{x}_8 z_{i+1} - \ddot{u}_g \\ 0 \\ \vdots \\ 0 \end{Bmatrix} \tag{21}$$

Equation (21) is a continuous state equation of the dynamic system. Using an appropriate measurement equation based on observed response quantities of the substructure ($u_i(t)$), the input quantity consisting of the external excitation $\ddot{u}_g(t)$, and the boundary response quantities, $z_{i+1}(t)$ and $z_{i-1}(t)$, the structural parameters can be identified by Kalman filter. Having identified the coefficients $\tilde{c}$ and $\tilde{k}$ the natural frequency and damping ratio of the substructure can be computed from below:

$$\tilde{k}_i = \frac{k_i}{m_i} = \omega_i^2$$
$$\tilde{c}_i = \frac{c_i}{m_i} = 2\xi_i\omega_i. \tag{22}$$

Case study of the local identification problem

The previous method was applied to identify the translation motion of T-section bridge–girder system (B1–A4–B2 section) described in Figure 7. In implementing the Kalman filtering procedure, initial values for the displacement and velocity were set at 0. The initial error covariance matrix was set at 0·1 for response and 100 for unknown parameters. The noise covariance matrix for the observation response was taken as 1·0. Shown in Table VI(a) and Table VI(b) are the results of the identification using the seismic reponse data of 23 February 1995 earthquake. In this substructural system only the parameters $\tilde{c}_i$, $\tilde{k}_i$, $\tilde{c}_{i+1}$, $\tilde{k}_{i+1}$, $\tilde{c}_{i-1}$ and $\tilde{k}_{i-1}$ can be obtained. Comparisions of the calculated response and observed response for m_i at node A4 and node B1 in transverse direction are shown in Figure 8. Since the local structural identification was performed there was no need to consider the quasi-static response contribution. A very good agreement in the predict response is obtained. Using the relationship between the substructure parameters the actual stiffness and damping of the subsystem will be discussed in the next section.

Discussion of the rigid-body rocking of pier–girder system

Consider the same pier–girder substructure system, as shown in Figure 9(a). It is assumed that the boundary excitations not only include the transverse motion at nodes 1–4 but also include the rotation in y-direction at

Table VI. (a) Estimated model parameters of the T-section (Pier: A4–C4, Girder: A4–B2, Girder: A4–B1) of New-Lian river bridge from both 1995-2-23 and 1995-6-25 earthquakes

Earthquake: transverse direction 23 Feb. 1995		
Pier: A4–C4 section	Girder: A4–B2 section	Girder: A4–B1 section
$k_i/m_i = 91{\cdot}333$	$k_{i-1}/m_i = 75{\cdot}473$	$k_{i+1}/m_i = 74{\cdot}459$
$c_i/m_i = 0{\cdot}8407$	$c_{i-1}/m_i = 0{\cdot}8889$	$c_{i+1}/m_i = 0{\cdot}7395$
Earthquake: transverse direction 25 June 1995		
$k_i/m_i = 91{\cdot}33$	$k_{i-1}/m_i = 75{\cdot}6353$	$k_{i+1}/m_i = 75{\cdot}6353$
$c_i/m_i = 1{\cdot}3923$	$c_{i-1}/m_i = 1{\cdot}2659$	$c_{i+1}/m_i = 1{\cdot}2659$

Table VI. (b) Estimated model parameters of the girder (Girder: B1–A4, Girder: B1–A3) of New-Lian River Bridge from 1995-2-23 earthquakes

Earthquake: transverse direction 23 Feb. 1995	
Girder: B1–A4 section	Girder: B1–A3 section
$k_i/m_i = 102{\cdot}31$	$k_{i+1}/m_i = 99{\cdot}12$
$c_{i-1}/m_i = 1{\cdot}2841$	$c_{i+1}/m_i = 1{\cdot}8303$

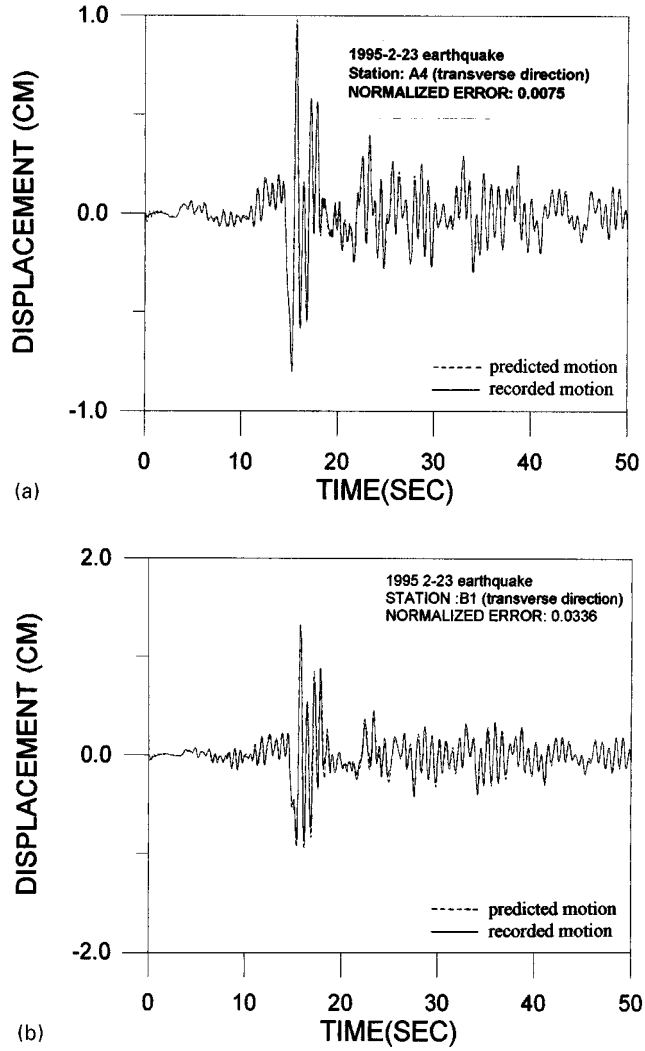

Figure 8. (a) Comparison of the predicted and recorded motions in transverse direction at station A4 for 1995-2-23 earthquake. The RMS error is 0·75%. (b) Comparison of the predicted and recorded motions in transverse direction at station B1 for 1995-2-23 earthquake. The RMS error is 3·36%

node 2 and rotation in x-direction at node 4 of the pier–girder system. In the discrete co-ordinate system assume the lumped mass matrix of the T-section of bridge–girder system can be obtained (from the design modal):

$$M = \begin{bmatrix} 1273 & 0 & 0 & 0 \\ 0 & 5651 & 0 & 0 \\ 0 & 0 & 1273 & 0 \\ 0 & 0 & 0 & 7905 \end{bmatrix} \times 10^3 \text{ kg} \tag{23}$$

This mass matrix M is obtained from the simplest procedure by considering the inertial properties and the actual dimension of the pier–girder system. The stiffness of the system can be obtained by applying unit displacement at each node and other nodes are assigned as fixed. Figure 9(b) shows the stiffness of k_{11} and k_{44} of the systems as

$$k_{11} = 4{\cdot}18 \times 10^8 \text{ N/m} \quad \text{and} \quad k_{44} = 5{\cdot}21 \times 10^8 \text{ N/m}$$

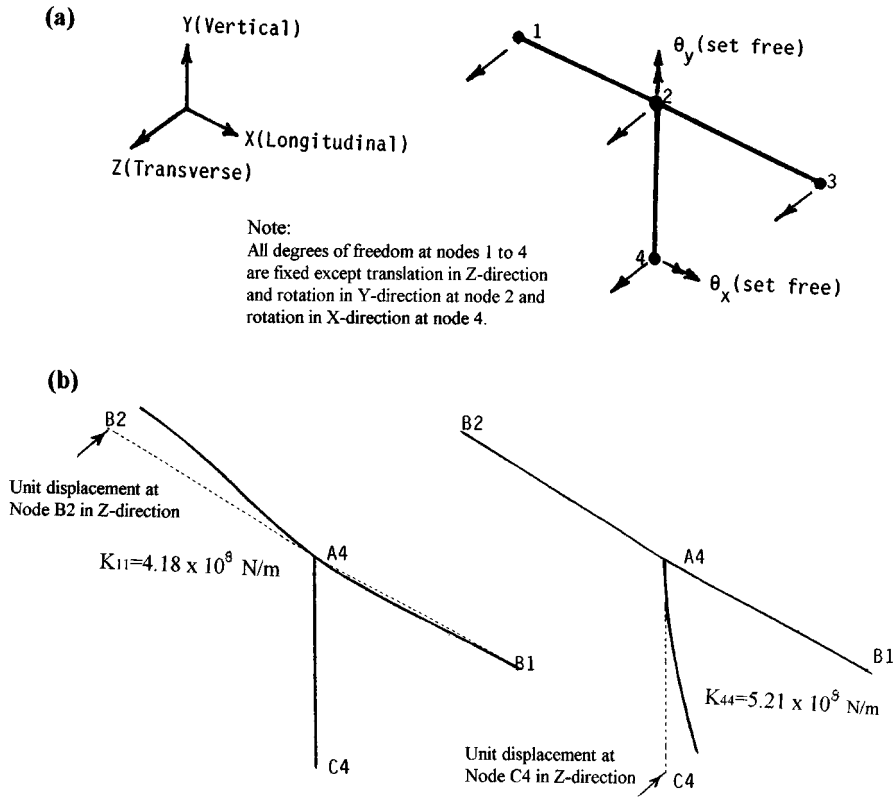

Figure 9. (a) Specified degrees of freedom at each node for the substructure system, (b) calculated stiffness K_{11} and K_{44} for the substructure system

From the result of identification, shown in Table VI(a), the pier stiffness can then be obtained by using the identified modal parameter $k_i/m_i = 91{\cdot}333$ N/kg m and multiplied by $m_i = 5{\cdot}651 \times 10^6$ kg to obtain the pier stiffness as

$$k_i = 91{\cdot}333 \times 5651 = 5{\cdot}161 \times 10^8 \text{ N/m}$$

This value is close to the designed stiffness of the pier ($k_{44} = 5{\cdot}21 \times 10^8$ N/m obtained by analytical treatment). Similar procedures can also be used to calculate the girder stiffness as

$$k_{i+1} = 74{\cdot}459 \times 5651 = 4{\cdot}208 \times 10^8 \text{ N/m}$$

This value is also close to the design stiffness ($k_{11} = 418060$ kNT/m). It is concluded that under 23 February 1995 earthquake the identified stiffness of the pier and girder are consistent with the design model.

During strong ground motion excitation (25 June 1995 earthquake) similar analysis and identification can be applied to the substructure system. Before the identification the rocking phenomenon of abutment was first examined using the recorded vertical motion at station C3 and C4. Figure 10 shows the calculated rocking of the pier foundation for 25 June 1995 earthquake. The rocking phenomenon is quite significant. To perform the identification of the pier–girder system shown in Figure 7 it is necessary to consider the rigid-body rocking in the recorded response of m_i so as to have an accurate identification of pier stiffness. Table VI(a) also shows the result of identification of the pier–girder system of A4–C4 section from 1996-6-25 earthquake. Similar results for the stiffness and damping were identified as compared to 23 February 1995 earthquake. Also shown in Tables VI(a) and (b), the identified damping of the pier is greater from the

response data of 25 June 1995 earthquake because of the larger response of the substructure system. Comparison between the predicted and the recorded response of mass m_i at nodes A4 in the transverse direction is shown in Figure 11. The restoring force diagram of transverse motion between nodes A4 and C4 for the two seismic events is also shown in Figure 12. It is clear that the larger hysteretic loop was observed from the response data of 25 June 1995 earthquake.

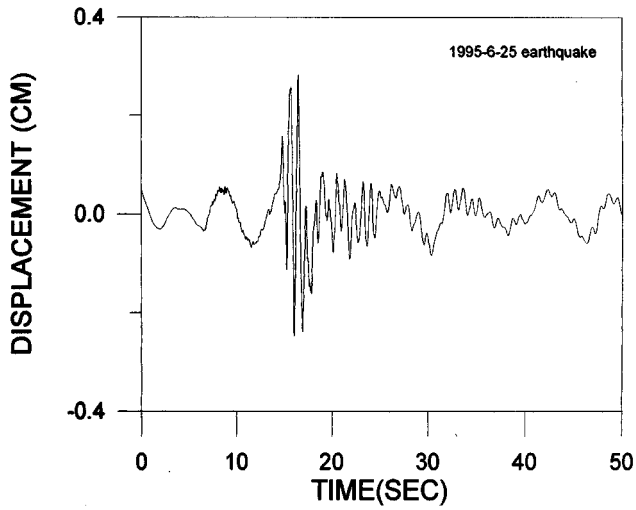

Figure 10. Differences of vertical displacement between stations C3 and C4 (rocking of foundation) for 1995-6-25 earthquake

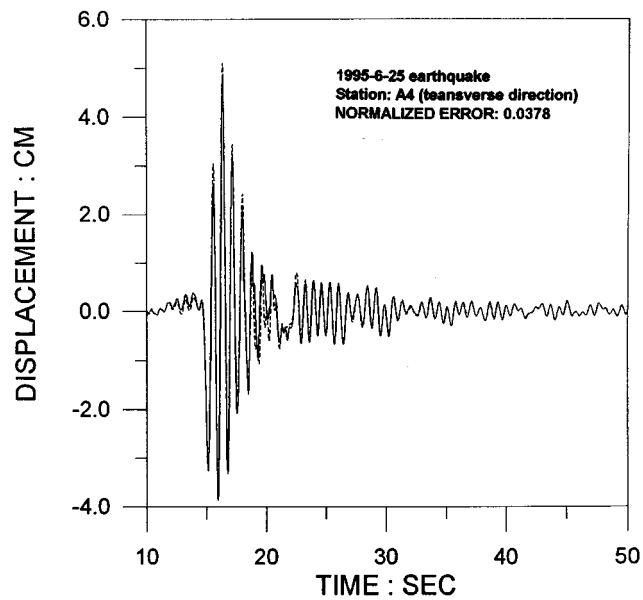

Figure 11. Comparison between the predicted (dash line) and the recorded (solid line) transverse motions at station A4. The kinematic interaction of pier–foundation is considered in the predicted motions. The RMS error is 3·78%

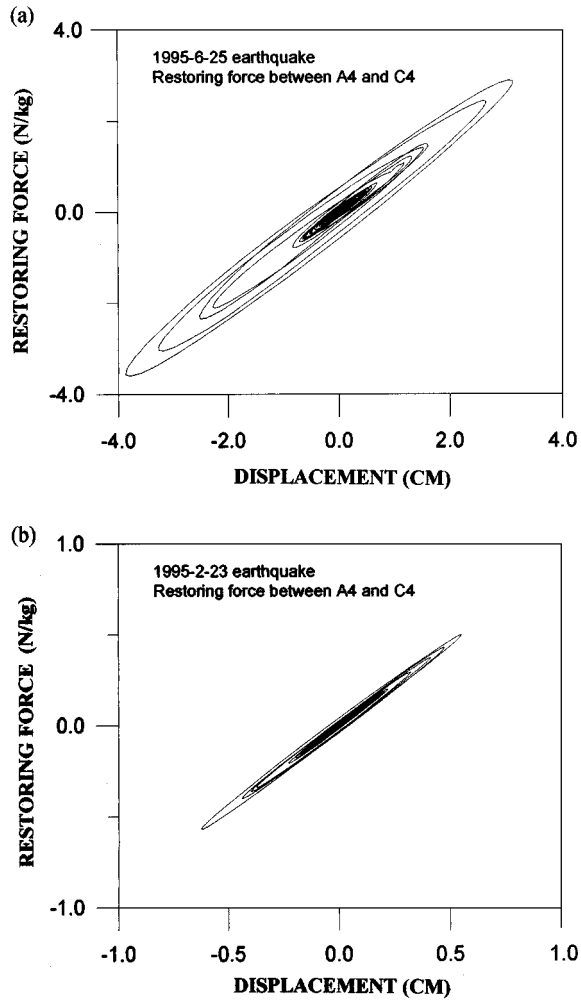

Figure 12. Restoring force diagram of girder motion between node A4 and C4 in transverse direction; (a) for 1995-6-25 earthquake, (b) for 1995-2-23 earthquake

Discussion on the transverse motion of the bridge girder

According to the analysis of the substructure system shown in Figure 13, the K-matrix and M-matrix shown in the appendix can be separated into the boundary system and the secondary system:

$$[K] = \begin{bmatrix} K_{ss} & K_{sb} \\ (2\times 2) & (2\times 4) \\ K_{bs} & K_{bb} \\ (4\times 2) & (4\times 4) \end{bmatrix} \quad \text{and} \quad [M] = \begin{bmatrix} M_{ss} & M_{sb} \\ (2\times 2) & (2\times 4) \\ M_{bs} & M_{ss} \\ (4\times 2) & (4\times 4) \end{bmatrix}$$

where u_j, θ_j, u_h and θ_h are the displacement and rotation from the boundary and u_i, θ_i are the motion and rotation of the subsystem. The equation of motion of the secondary system is expressed as[10]

$$M_{ss}\ddot{u}_s^d + C_{ss}\dot{u}_s^d + K_{ss}u_s^d = [M_{ss}K_{ss}^{-1}K_{sb} - M_{sb}]\ddot{u}_b^t$$

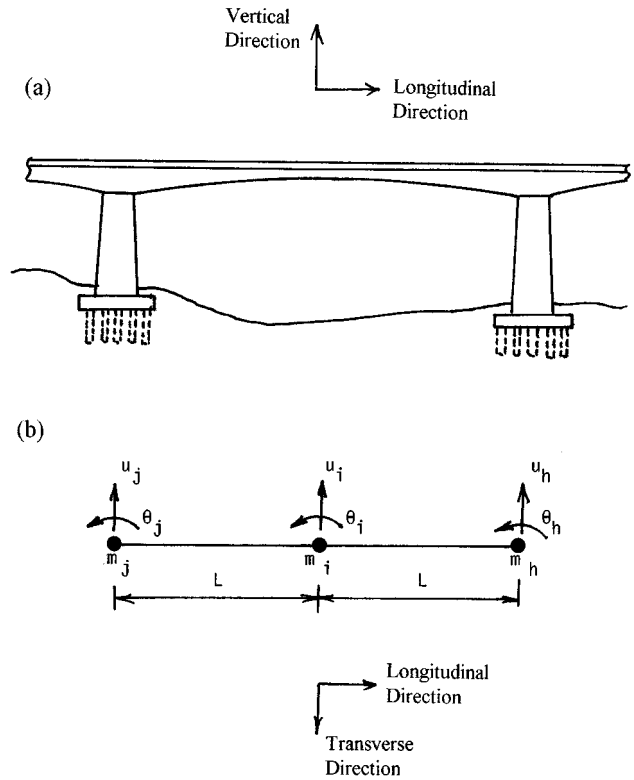

Figure 13. (a) A bridge–girder substructure system between two piers, (b) lumped mass model indicated degrees of freedom at each node

where $u_b^t = \langle u_j, \theta_j, u_h, \theta_h \rangle$. u_j and u_h can be collected from the measurements and θ_j and θ_h can be calculated through the spline approximation of the detected motion in the transverse direction. Generally, the displacement of the substructure system can be expressed as the sum of quasi-static displacement and dynamic response as indicated:

$$u_s = u_s^d + u_s^{qs}$$

where u_s^{qs} is the quasi-static displacement ($u_s^{qs} = -K_{ss}^{-1} K_{sb} u_b = -R u_b(t)$). Taking as an example of the transverse motion of node i in Figure 13(b), the equation of motion of m_i in the transverse direction can be expressed as

$$\left(\frac{13\,dl}{35}\right)\ddot{u}_{si}^d + c_s \dot{u}_{si}^d + \frac{193EI}{l} u_{si}^d = [M_{ss} K_{ss}^{-1} K_{sb} - M_{sb}] \begin{Bmatrix} \ddot{u}_j \\ \ddot{\theta}_j \\ \ddot{u}_h \\ \ddot{\theta}_h \end{Bmatrix} \tag{24}$$

The quasi-static response of the bridge–girder substructure system is expressed as $u_s^{qs} = -R u_b$, and

$$u_s^{qs} = \begin{Bmatrix} u_i \\ \theta_i \end{Bmatrix}^{qs}, \qquad R = \begin{bmatrix} -1/2 & -1/8l & -1/2 & 1/8l \\ 3/2l & 1/4 & -3/2l & 1/4 \end{bmatrix} \quad \text{and} \quad u_b = \begin{Bmatrix} u_j \\ \theta_j \\ u_h \\ \theta_h \end{Bmatrix}_b \tag{25}$$

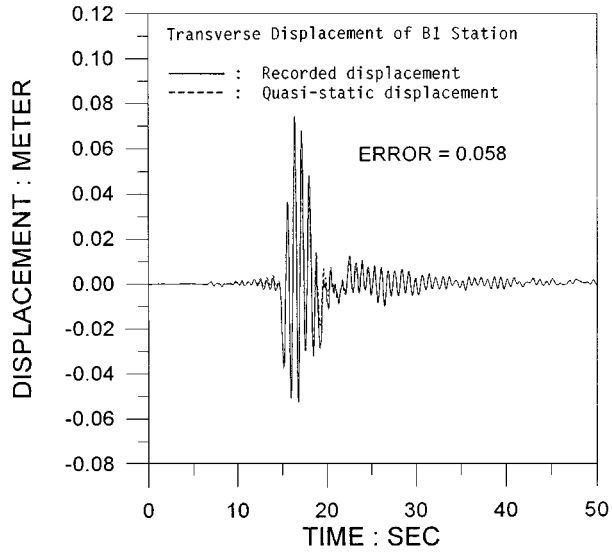

Figure 14. Comparison between the recorded motion (solid line) and the quasi-static displacement (dash line) of station B1 for 1995-6-25 earthquake

and u_b is the displacement field at the boundary system. The quasi-static response of the substructural system can be calculated through equation (32). Consider the transverse motion of node B1 as an example of this analysis. Figure 14 shows the comparison between the recorded motion and the predicted response of the quasi-static response of node B1 in transverse motion. A very good agreement on the response was observed. It is concluded that the contribution of the quasi-static response from the boundary system (include rotation and translation at nodes A4 and A3) will have a significant effect on the response of node B1 in transverse direction. The quasi-static contribution is obvious for the seismic response data of 25 June 1995 earthquake.

CONCLUSIONS

This paper shows the structural system identification of the seismic response measurements from an array of strong-motion instruments. The results show that the classical dynamic model of structures identified from the New-Lian river bridge's strong-motion measurements have provided a good representation of its seismic response characteristics. Some important practical results that should be useful in the future seismic design of bridges include the following:

(a) *Effects of rigid-body rotation of abutment in transverse direction*
Differences between weak motion and strong motion on the response of bridge piers is the contribution of rigid-body rotation of the abutment induced by strong ground motion. During strong motion (such as 25 June 1995 earthquake) the rotation of the abutment may induce a large displacement at the top of the pier. In order to identify the dynamic characteristics of the structural system, this rigid-body rotation of abutment must be considered in the identification analysis.

(b) *Damping ratios*
From the analysis of the response data of the bridge system subjected to two different level of seismic excitations, the damping ratio of pier will increase from 4·39 per cent for 23 February 1995 earthquake to 7·28 per cent for 25 June 1995 earthquake. The dynamic behaviour of the bridge pier is still in the linear elastic range when subjected to these two seismic excitations. The damping ratio of the bridge girder in transverse direction will increase from 6·34 to 10·83 per cent under the different level of excitations.

(c) *Quasi-static contribution in the transverse motion of the bridge girder*
From the dynamic response analysis of the bridge girder it is found that during strong excitation the quasi-static response will dominate the response of the bridge girder. On the contrary for small ground excitation the contribution of dynamic term will dominate the response. Of course, this conclusion may depend on the foundation condition.

(d) *Dynamic stiffness levels*
Dynamic analysis using simplified finite element models as well as using system identification provide insights into the nature of the dynamic stiffness developed in the NLRB during earthquake. The evaluation indicates that the estimated pier stiffness during the earthquake is within the design level (from analysis). Although 25 June 1995 earthquake induced large acceleration on the response of the bridge but the stress in the pier was not increased because the earthquake-induced translational and rotational motions of the abutment was considered.

In addition to the above-mentioned results this research provides the method for local structural system identification. Although the linear model was used in the current study, the future use of non-linear models can be extended if larger input motion was obtained.

ACKNOWLEDGEMENTS

The seismic response data provided by the Seismological Observation Centre, Central Weather Bureau, Taiwan, is gratefully acknowledged. The project was founded through grants by Taiwan Area National Freeway Bureau and by Central Weather Bureau, Ministry of Transportation and Communications, whose financial support is gratefully acknowledged.

APPENDIX

Consider different local substructure system of a bridge girder, as shown in Figure 13. Assuming a uniform beam segment the end displacements and forces are induced as follows (this assumption did not cause significant difference as compared to the design model):

$$\begin{bmatrix} F_{v_1} \\ F_{\theta_1} \\ F_{v_2} \\ F_{\theta_2} \end{bmatrix} = \frac{8EI}{l^3} \begin{bmatrix} 12 & 3l & -12 & 3l \\ 3l & l^2 & -3l & l^2/2 \\ -12 & -3l & -12 & 3l \\ 3l & l^2/2 & -3l & l^2 \end{bmatrix} \begin{Bmatrix} v_1 \\ \theta_1 \\ v_2 \\ \theta_2 \end{Bmatrix} \tag{26}$$

where v_1, θ_1 indicate the translation and rotation degrees of freedom at node 1, and $v_2\theta_2$ indicate the translation and rotation degrees of freedom at node 2. The consistent mass matrix is

$$[M] = \frac{ml}{840} \begin{bmatrix} 156 & 11l & 54 & -6{\cdot}5l \\ 11l & l^2 & 6{\cdot}5l & -0{\cdot}75l^2 \\ 54 & 6{\cdot}5l & 15{\cdot}6 & -11l \\ -6{\cdot}5l & -0{\cdot}75l^2 & -11l & l^2 \end{bmatrix} \tag{27}$$

where m is the density of the material and l is the length of the beam element. For the analysis of such a bridge–girder system, with the lumped mass model shown in Figure 13, the force–displacement relationship

and the mass matrix of the system are indicated (combining two beam elements):

$$\begin{Bmatrix} F_{v_1} \\ M_{\theta_1} \\ F_{v_2} \\ M_{\theta_2} \\ F_{v_3} \\ M_{\theta_3} \end{Bmatrix} = \begin{bmatrix} \frac{192EI}{l^3} & 0 & \frac{-96EI}{l^3} & \frac{-24EI}{l^2} & \frac{-96EI}{l^3} & \frac{24EI}{l^2} \\ 0 & \frac{16EI}{l} & \frac{24EI}{l^2} & \frac{4EI}{l} & \frac{-24EI}{l^2} & \frac{4EI}{l} \\ \frac{-96EI}{l^3} & \frac{24EI}{l^2} & \frac{96EI}{l^3} & \frac{24EI}{l^2} & 0 & 0 \\ \frac{-24EI}{l^2} & \frac{4EI}{l} & \frac{24EI}{l^2} & \frac{8EI}{l} & 0 & 0 \\ \frac{-96EI}{l^3} & \frac{-24EI}{l^2} & 0 & 0 & \frac{96EI}{l^3} & \frac{-24EI}{l^3} \\ \frac{24EI}{l^2} & \frac{4EI}{l} & 0 & 0 & \frac{-24EI}{l^2} & \frac{8EI}{l} \end{bmatrix} \begin{Bmatrix} v_1 \\ \theta_1 \\ v_2 \\ \theta_2 \\ v_3 \\ \theta_3 \end{Bmatrix} \tag{28}$$

where $v_1 = u_i$, $\theta_1 = \theta_i$, $v_2 = u_j$, $\theta_2 = \theta_v$, $v_3 = u_h$, $\theta_3 = \theta_h$, and F denotes force, M denotes moment, as indicated in Figure 13(b), and the mass matrix of the system is expressed as

$$M = \begin{bmatrix} \frac{13ml}{35} & 0 & \frac{9ml}{140} & \frac{13ml^2}{1680} & \frac{9ml}{140} & \frac{-13ml^2}{1680} \\ 0 & \frac{ml^3}{420} & \frac{-13ml^2}{1680} & \frac{-ml^3}{1120} & \frac{13ml^2}{1680} & \frac{-ml^3}{1120} \\ \frac{9ml}{140} & \frac{-13ml^2}{1680} & \frac{13ml}{70} & \frac{11ml^2}{840} & 0 & 0 \\ \frac{13ml^2}{1680} & \frac{-ml^3}{1120} & \frac{11ml^2}{840} & \frac{ml^3}{840} & 0 & 0 \\ \frac{9ml}{140} & \frac{13ml^2}{1680} & 0 & 0 & \frac{13ml}{70} & \frac{-11ml^2}{840} \\ \frac{-13ml^2}{1680} & \frac{-ml^3}{1120} & 0 & 0 & \frac{-11ml^2}{840} & \frac{ml^3}{840} \end{bmatrix} \tag{29}$$

REFERENCES

1. Northridge Earthquake of January 17, in *1994 Reconnaissance Report*, Vol. 1, J. F. Hall (ed.), Earthquake Spectra, EERI, April 1995.
2. The Hyogo-Ken Nanbu Earthquake, January 17, 1995, in *Preliminary Reconnaissance Report*, C. D. Comartin, M. Greene and S. K. Tubbesing (eds), Earthquake Engineering Research Institute, February, 1995.
3. Public Works Research Institute, 'A case history of bridge performance during earthquakes in Japan', *Proc. int. conf. case hist. geotech. eng.*, St. Louis, MO, 1984.
4. B. D. Douglas *et al.*, *Behavior of the Meloland Road Overcrossing During the 1979 Imperial Valley Earthquake*, Seismic Research for Highway Bridge, Univ. of Pittsburgh, PA, 1984, pp. 339–365.
5. J. C. Wilson, 'Analysis of the observed earthquake response of a multiple span bridge', *EERL Report No. 84-01*, California Institute of Technology, Pasadena.
6. S. D. Werner, J. L. Beck and M. B. Levin, 'Seismic response evaluation of Meloland road overpass using 1979 Imperial Valley Earthquake Records', *Earthquake eng. struct. dyn.* **15**, 249–274 (1987).
7. T. Söderstrm̈, *Petre Stoica*, *System Identification*, Prentice-Hall, Englewood Cliffs, NJ, 1989.
8. W. Gersch and S. Luo, 'Discrete time series synthesis of randomly excited structural system response', *J. acoust. soc. Am.* **51**, 402–408 (1972).
9. A. DerKiureghian and A. N. Hofer, 'Response spectrum method for multi-support seismic excitations', *Earthquake eng. struct. dyn.* **21**, 713–740 (1992).
10. A. W. C. Oreta, 'Development of method of identification of local structural parameters by Kalman filter', *Ph.D. dissertation*, Nagiya University, Japan, March 1994.
11. C. H. Loh, J. Penzien and Y. B. Tsai, 'Engineer analysis of SMART-1 seismic data', *Earthquake eng. struct. dyn.* **10**, 575–591 (1982).